OPEN

NPG Asia Materials (2015) 7, e230; doi:10.1038/am.2015.126
www.nature.com/am

ORIGINAL ARTICLE

Self-assembled multicolor nanoparticles based on functionalized twistacene dendrimer for cell fluorescent imaging

Xuemin Zhang[1,3], Shengliang Li[2,3], Zhenying Liu[1], Shu Wang[2] and Jinchong Xiao[1]

A series of twistacene-functionalized dendrimers were successfully synthesized and characterized. The model molecule DBPy has a twisted configuration with a torsional angle of 27.69° between pyrene and naphthalene units. The resulting compounds TPPh, TTPy, OTPy and TOPhP can self-assemble into organic nanoparticles through re-precipitation method and emit strong blue, cyan, green and red fluorescence in water, respectively. Additionally, the obtained multicolor nanoparticles showed low cytotoxicity and good photostability that selectively flow into the membrane and cytoplasm of HeLa cells, indicating the feasibility and efficiency in fluorescence imaging. This study might be a new avenue for the design of three-dimensional branched conjugated molecule and specific location imaging in living cell.

NPG Asia Materials (2015) **7,** e230; doi:10.1038/am.2015.126; published online 18 December 2015

INTRODUCTION

Supramolecular assembly of organic conjugated small and polymers has become one of the most active research topics during the past two decades, because the performance of organic soft devices mainly depends on the molecular design, intermolecular interaction, ordered packing and optoelectronic properties to a great extent.[1–9] In general, these molecules can self-assemble into different microstructures/nanostructures such as spheres, bars, wires, tubes and vesicles, and these ordered aggregations were used as key active layers in material science. More recently, they also presented high selectivity and sensitivity used as bioprobes because the dimensionally controllable skeletons showed extraordinary physical properties over the corresponding single molecule.[10–15] As known, in order to intensively realize the nucleus modification and diagnostic, prognostic information, fluorescence cell imaging has matured into a novel platform in recent years.[16–22] For example, Misra and co-workers prepared some highly photoluminescent semiconductor quantum dots based on ZnO that could be immobilized of HeLa cells, which was beneficial for detecting the cancer cells in cell therapy.[23–25] However, the appropriate fluorescent biomaterials that can enter and deposit into the special cellular position are still limited, considering the photostability, cytotoxicity and permeability, which encourages us to prepare microstructures/nanostructures with tuning size and shape based on organic conjugated molecules.

Acenes, usually consisting of a series of fused linear benzologs, are the subjects of considerable investigations because of their extraordinary electronic structure, fascinating physical property and the potential application in organic soft electronics.[26–31] When one phenanthrene or pyrene units are grafted into the acenes in the terminal, the formed molecules can twist owing to the steric hindrance, which might be beneficial for application as active layers in organic light emitting diodes because this conformation can decrease the stacking interaction to a certain extent.[32–34] Wudl, Zhang and Xiao synthesized a series of symmetric and asymmetric twistacenes containing primary color luminescence from blue to green and red through retro-Dies-Alder reaction.[35–40] It is well known that well-defined conjugated dendrimers having branched and regularly repeating molecular units possess many advantages over small molecules and the hyperbranched polymers. The optoelectronic properties of these dendrimers can be finely tuned by changing the core, decorating with various surface groups and grafting with different functional generations. For example, Müllen and co-workers synthesized some polyphenylene dendrimers with different central cores and tested their physical property.[41–43] The group of Pei developed a new class star-shaped dendrimers based on truxene that could be used as promising candidates for light-harvesting materials.[44–46] When twistacenes are implanted into the three-dimensional architectures, the as-formed novel dendrimers can effectively suppress intramolecular and intermolecular π–π stacking in

[1]College of Chemistry and Environmental Science, Key Laboratory of Chemical Biology of Hebei Province, Hebei University, Baoding, PR China and [2]Beijing National Laboratory for Molecular Sciences, Key Laboratory of Organic Solids, Chinese Academy of Sciences, Beijing, PR China
[3]These authors contributed equally to this work.
Correspondence: Professor S Wang, Beijing National Laboratory for Molecular Sciences, Key Laboratory of Organic Solids, Chinese Academy of Sciences, No 2, Zhongguancun North First Street, Beijing 100190, PR China.
E-mail: wangshu@iccas.ac.cn
or Professor J Xiao, College of Chemistry and Environmental Science, Key Laboratory of Chemical Biology of Hebei Province, Hebei University, Baoding 071002, PR China.
E-mail jcxiaoicas@163.com
Received 4 August 2015; revised 24 September 2015; accepted 29 September 2015

high concentration solution and solid state without sacrificing other physical property. Nevertheless, current researches mainly focus on the synthesis and application of these derivatives in organic devices. The approach to fabricate the microstructures/nanostructures based on these π-conjugated dendrimers remains challenging and scarce until now, which strongly stimulates us to induce their self-assembly, tune the optoelectronic properties and investigate the effect of molecular topology on the cell imaging.

In this work, we describe the design, synthesis and self-assembly of the biology of several π-conjugated dendrimers (Scheme 1). **TPPh**, **TTPy**, **OTPy** and **TOPhP** can form uniform nanoparticles by using a re-precipitation method with blue, cyan, green and red luminescence under single excitation wavelength, respectively. These nanoparticles exhibited good photostability and low biological cytotoxicity. More interesting, such dendrimer-fabricated nanoparticles can selectively implant the membrane and cytoplasm of HeLa cells depending on their structural properties. Clearly, this systematic study provides a new platform for the construction of nanostructures by controlling optoelectronic property and biological affinity.

MATERIALS AND METHODS

Materials and characterization

The chemicals were utilized as received from commercial companies. ^{1}H nuclear magnetic resonance (NMR) and ^{13}C NMR spectra were recorded on Bruker AVANCE 600 MHz digital NMR spectrometer (Fällanden, Switzerland) with $CDCl_3$ as a solvent without any internal standard. Matrix-assisted laser desorption ionization time of flight (MALDI-TOF) mass spectrometric measurements were measured on Bruker Biflex III MALDI-TOF (Billerica, MA, USA). UV-Vis absorption and fluorescence spectra were carried out on Shimadzu UV-2550 and RF5300PC spectrometers (Kyoto, Japan). Scanning electron microscopy (SEM) characterization was achieved by a field-emission SEM (FESEM) (JSM-7500F, JEOL, Tokyo, Japan) at an accelerating voltage of 10 kV. The size distributions and zeta potential of the nanoparticles were also characterized by dynamic light scattering method with a Nano ZS90 system (Malvern Instruments Ltd, Malvern, UK). Thermalgravimetric analysis was recorded on a Perkin-Elmer thermal analyzer (Pyris 6, Boston, MA, USA). X-ray crystallographic data were obtained by using a Bruker smart APEX II CCD diffractometer (Karlsruhe, Germany) with a graphite-monochromatic Mo Kα radiation ($\lambda = 0.71073$ Å) at 296 K. Ultrapure water was prepared by Millipore S.A. 67120 appratus with a resistivity of 18.2 MΩ cm^{-1}.

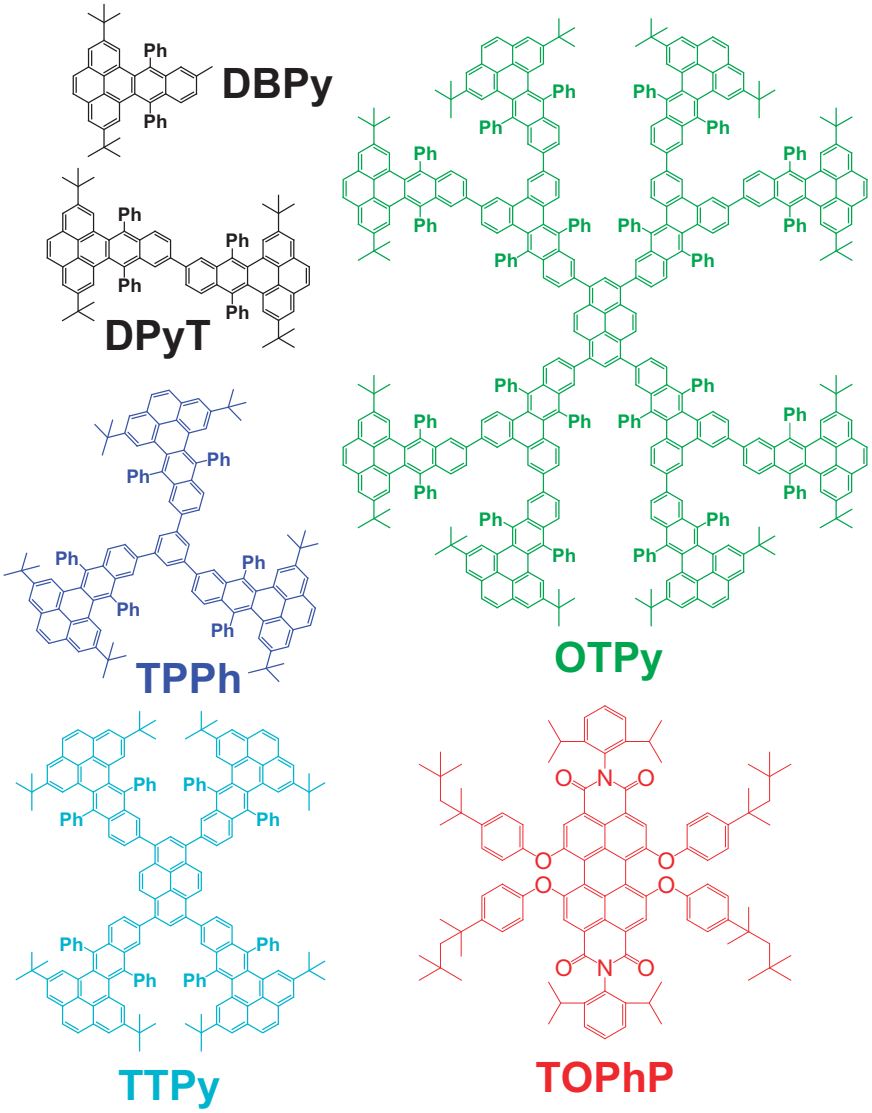

Scheme 1 Molecular structures of **DBPy** (**6**, black), **DPyT** (**11**, black), **TPPh** (blue), **TTPy** (**12**, cyan), **OTPy** (**18**, green) and **TOPhP** (red).

Compound **3**: 2,7-Di-*tert*-butyl-pyrene-4,5-dione (**1**, 700 mg, 2.03 mmol) and 1,3-diphenylacetone (**2**, 475 mg, 2.26 mmol) were dispersed into ethanol (30 ml). A mixture solution of KOH (105 mg) in methanol (2.0 ml) was added dropwise slowly. The solution was stirred and heated in refluxing temperature for 15 min. The reaction mixture was cooled to room temperature, successively washed with brine solution and extracted with methylene chloride (30 ml × 3). The organic phase was collected and concentrated under reduced pressure. The obtained residue was further purified by column chromatography with methylene chloride/petroleum ether (v/v, 1:7) to afford compound **3** (black solid, 449 mg, 43%). ^{1}H NMR (600 MHz, $CDCl_3$, 298 k): $\delta = 7.92$ (d, 2 H), 7.66 (d, 2 H), 7.60 (s, 2 H), 7.50–7.46 (m, 8 H), 7.42–7.39 (m, 2 H), 1.13 (s, 18 H). ^{13}C NMR (150 MHz, $CDCl_3$, 298 K): $\delta = 200.59$, 149.60, 148.57, 133.11, 131.98, 130.03, 128.79, 128.00, 127.12, 127.09, 126.71, 126.52, 124.84, 123.50, 34.61, 30.84. MS (MALDI-TOF): Calc. for $C_{39}H_{34}O$: [M] 518.26, found: [M+1] 519.2, [M+Na$^+$] 541.2.

Compound **6** (**DBPy**): 2-Amino-5-methylbenzoic acid (**4**, 320 mg, 2.1 mmol) dispersed in 1,2-dichloroethane (DCE) solution and isoamyl nitrile (2.5 ml) were added alternatively into a mixture solution of 2,7-di-tert-butyl-9,10-diphenyl-10H-cyclopenta[e]pyren-10-one (**3**, 1.0 g, 1.9 mmol), which was preheated at 90 °C in DCE (40 ml). The reaction mixture was stirred and kept at 90 °C for 12 h. After cooling to room temperature, brine and methylene chloride was added. The organic phase was collected and concentrated under reduced pressure. The crude product was further purified through column chromatography on silica gel using petroleum ether to give compound **6** (light yellow solid, 120 mg, 11%). ^{1}H NMR (600 MHz, $CDCl_3$, 298 k): $\delta = 8.13$ (s, 2 H), 7.84 (s, 2 H) 7.83 (s, 2 H), 7.76 (d, $J = 12.0$ Hz, 1 H), 7.61–7.55 (m, 9 H), 7.47–7.45 (m, 2 H), 7.29 (d, $J = 12.0$ Hz, 2 H), 2.46 (s, 3 H), 1.12 (s, 18 H). ^{13}C NMR (150 MHz, $CDCl_3$, 298 K): $\delta = 147.21$, 147.17, 142.88, 142.86, 136.05, 135.51, 135.27, 132.52, 132.43, 132.28, 130.54, 130.32, 130.30, 129.82, 129.78, 129.26, 128.85, 127.99, 127.67, 127.47, 127.40, 127.39, 126.92, 126.91, 126.73, 125.47, 123.92, 123.82, 122.12, 121.99, 34.78, 31.44, 31.43, 32.05. MS (MALDI-TOF): Calc. for $C_{45}H_{40}$: [M] 580.31, found: [M] 580.3.

Compound **7**: 2-Amino-5-bromobenzoic acid (**5**, 250.0 mg, 1.16 mmol) dispersed in DCE solution and isoamyl nitrile (1.2 ml) in DCE (25 ml) were added alternatively into a mixture solution of compound **3** (580.0 mg, 1.12 mmol), which was preheated at 90 °C in DCE. After 12 h, the reaction mixture was cooled to room temperature, washed with brine and extracted with methylene chloride (30 ml × 3). The organic phase was separated and concentrated under reduced pressure. The crude product was further purified through column chromatography using petroleum ether as eluent to give compound **7** (light yellow solid, 203 mg, 28%). ^{1}H NMR (600 MHz, $CDCl_3$, 298 k): $\delta = 8.12$ (t, 2 H), 7.98, (S, 1 H), 7.84 (S, 4 H), 7.71 (d, $J = 12.0$ Hz, 1 H), 7.57–7.55 (m, 8 H), 7.49–7.47 (m, 3 H), 1.11 (s, 18 H). ^{13}C NMR (150 MHz, $CDCl_3$, 298 K): $\delta = 147.36$, 147.35, 142.05, 136.21, 135.25, 133.23, 132.33, 130.86, 130.57, 130.37, 130.34, 130.07, 129.55, 129.44, 129.34, 129.28, 128.84, 128.78, 128.65, 127.84, 127.76, 127.73, 127.61, 126.98, 123.89, 122.62, 122.51, 120.22, 34.80, 31.42. MS (MALDI-TOF): Calc. for $C_{44}H_{37}Br$: [M] 645.67, found: [M+1] 646.5.

Compound **9**: $Pd(dppf)_2Cl_2$ (25 mg, 0.031 mmol) was added to a mixture of compound **7** (400 mg, 0.62 mmol), bis(pinacolato)diboron (**8**, 253 mg, 1 mmol), potassium acetate (365 mg, 3.72 mmol) and dry DMF (20 ml) in nitrogen atmosphere. The reaction solution was stirred and kept at 90 °C for 24 h. After cooling to room temperature, brine and methylene chloride were added. The organic phase was collected and dried with anhydrous sodium sulfate. After removal the solvent, the residue was further purified with on silica gel with ethyl acetate/petroleum ether (v/v, 1:50) to afford compound **9** (yellow solid, 321 mg, 75%). ^{1}H NMR (600 MHz, $CDCl_3$, 298 k): $\delta = 8.41$ (s, 1 H), 8.13 (s, 1 H), 8.08 (s, 1 H), 7.84 (d, $J = 6.0$ Hz, 4 H), 7.79 (s, 2 H), 7.61–7.54 (m, 8 H), 7.49–7.45 (m, 2 H), 1.35 (s, 12 H), 1.12 (s, 18 H). ^{13}C NMR (150 MHz, $CDCl_3$, 298 K): $\delta = 147.23$, 147.20, 142.65, 142.24, 136.95, 135.85, 134.96, 132.71, 132.50, 130.30, 130.27, 130.06, 129.57, 129.25, 129.16, 127.66, 127.57, 127.44, 126.91, 125.68, 123.98, 123.82, 122.34, 122.12, 83.75, 34.75, 31.39, 24.88. MS (MALDI-TOF): Calc. for $C_{50}H_{49}BO_2$: [M] 692.38, found: [M] 692.4.

Compound **11**: A mixture of compound **7** (92 mg, 0.15 mmol), **9** (105 mg, 0.15 mmol), $Pd(PPh_3)_4$ (10 mg, 0.008 mmol) and Na_2CO_3 (300 mg) was stirred in tetrahydrofuran (THF)/H_2O (25 ml per 4 ml) at 70 °C under nitrogen atmosphere. After 2 d, the solution was cooled to room temperature. The solution was diluted with dichloromethane (80 ml), washed with brine (50 ml × 3) and dried over sodium sulfate. The organic extracts were removed under reduced pressure. The formed residue was further purified through column chromatography on silica gel by using petroleum/dichloromethane (v/v, 25:1) to afford **11** (green solid, 68%). ^{1}H NMR (600 MHz, $CDCl_3$, 298 k): $\delta = 8.17$ (t, $J = 1.2$ Hz, 4 H), 8.15 (d, $J = 1.8$ Hz, 2 H), 7.92 (s, 1 H) 7.90 (s, 1 H), 7.85–7.84 (m, 8 H), 7.73 (d, $J = 1.8$ Hz, 1 H), 7.72 (d, $J = 1.8$ Hz, 1 H), 7.63–7.57 (m, 12 H), 7.55 (t, $J = 7.8$ Hz, 4 H), 7.50–7.46 (m, 4 H), 1.13 (s, 18 H), 1.12 (s, 18 H). ^{13}C NMR (150 MHz, $CDCl_3$, 298 K): $\delta = 147.30$, 147.27, 142.71, 142.54, 137.77, 136.48, 135.98, 132.46, 132.41, 130.33, 130.25, 129.87, 129.64, 129.35, 129.33, 127.71, 127.61, 127.57, 127.52, 127.49, 126.93, 125.10, 124.91, 123.94, 123.90, 122.27, 122.22, 34.78, 31.41. MS (MALDI-TOF): Calc. for $C_{88}H_{74}$: [M] 1130.58, found: [M+1] 1130.7.

Compound **12**: A mixture of compound **9** (321 mg, 0.468 mmol), 1,3,6,8-tetrabromopyrene (**10**, 42 mg, 0.081 mmol), $Pd(PPh_3)_4$ (50 mg, 0.043 mmol) and K_2CO_3 (110 mg, 0.79 mmol) in toluene/ethanol/H_2O (15 ml, v/v/v, 8:1:1) was stirred in refluxing temperature for 16 h in nitrogen atmosphere. After cooling to room temperature, brine was added to the reaction solution, which was further extracted with methylene chloride (50 ml × 3). The organic phase was collected, dried with anhydrous sodium sulfate and then concentrated under reduced pressure. The obtained product was further purified through silica gel column chromatography using methylene chloride/petroleum ether (v/v, 1:100) as the eluent to afford **12** (**TTPy**, yellow solid, 86 mg, 45%). ^{1}H NMR (600 MHz, $CDCl_3$, 298 k): $\delta = 8.34$ (s, 4 H), 8.23 (d, 4 H), 8.20 (s, 8 H), 8.14 (s, 2 H), 8.12 (d, $J = 12.0$ Hz, 4 H), 7.87–7.85 (t, 16 H), 7.81 (d, $J = 12.0$ Hz, 4 H), 7.75 (d, $J = 6.0$ Hz, 8 H), 7.69 (d, $J = 6.0$ Hz, 8 H), 7.62 (t, 8 H), 7.52 (t, 4 H), 7.46, (t, 8 H), 7.33 (t, 4 H), 1.15 (s, 36 H), 1.12 (s, 36 H). ^{13}C NMR (150 MHz, $CDCl_3$, 298 K): $\delta = 147.32$, 147.30, 142.71, 142.43, 138.21, 137.42, 136.48, 136.08, 132.54, 132.45, 132.06, 131.89, 131.28, 131.26, 130.36, 130.34, 130.04, 129.91, 129.64, 129.40, 128.81, 128.45, 128.43, 128.41, 127.73, 127.62, 127.58, 127.01, 126.96, 126.00, 125.60, 125.59, 123.96, 123.95, 122.32, 122.30, 34.81, 34.79, 31.43. MS (MALDI-TOF): Calc. for $C_{192}H_{154}$: [M] 2459.21, found: [M+1] 2460.7.

Compound **15**: 2-Amino-5-iodobenzoic acid (**14**, 162 mg, 0.6 mmol) dispersed in DCE (10 ml) solution and isoamyl nitrile (1 ml) were added alternatively into a mixture solution of **13** (333 mg, 0.6 mmol), which was preheated at 90 °C in DCE (10 ml). The reaction mixture was stirred and kept at 90 °C overnight. After cooling to room temperature, brine (60 ml) was added and the mixture was extracted with methylene chloride (30 ml × 3). The organic phase was collected and concentrated. The obtained crude product was purified through column chromatography on silica gel using petroleum ether/CH_2Cl_2 (v/v: 8:1) to give **15** (light yellow solid, 348 mg, 81%). ^{1}H NMR (600 MHz, $CDCl_3$, 298 k): $\delta = 8.30$ (d, $J = 2.4$ Hz, 2 H), 8.27 (d, $J = 1.8$ Hz, 1 H), 7.70 (dd, $J^1 = 9.0$ Hz, $J^2 = 1.8$ Hz, 1 H), 7.62 (d, $J = 9.0$ Hz, 1 H), 7.57–7.52 (m, 6 H), 7.49–7.47 (m, 4 H), 7.33 (t, $J = 9.0$ Hz, 2 H), 7.10 (dd, $J^1 = 9.0$ Hz, $J^2 = 1.2$ Hz, 2 H). ^{13}C NMR (150 MHz, $CDCl_3$, 298 K): $\delta = 140.56$, 140.41, 135.88, 135.39, 134.64, 134.61, 133.42, 132.66, 132.59, 132.33, 132.29, 132.01, 131.91, 130.71, 130.20, 130.18, 129.47, 129.46, 129.36, 128.18, 128.47, 128.29, 128.19, 126.21, 126.20, 121.66, 121.59, 92.75. MS (MALDI-TOF): Calc. for $C_{34}H_{19}Br_2I$: [M] 714.2, found: [M] 714.0.

Compound **17**: A mixture of compound **15** (619 mg, 0.87 mmol), **16** (100 mg, 0.14 mmol), $Pd(PPh_3)_4$ (190 mg, 0.164 mmol) and $NaHCO_3$ (300 mg) in THF/H_2O (20 ml per 4 ml) was stirred at 70 °C for 8 days under nitrogen atmosphere. After cooling to room temperature, brine was added to the reaction solution, which was further extracted with methylene chloride (60 ml × 3). The organic phase was collected and then removed under reduced pressure. The resulting residue was further purified through silica gel column chromatography using methylene chloride/petroleum ether (v/v, 1:8) as the eluent to give **17** (light yellow solid, 135 mg, 37%). ^{1}H NMR (600 MHz, $CDCl_3$, 298 k): $\delta = 8.32$ (s, 8 H), 8.21 (s, 4 H), 8.19 (s, 3 H), 8.12 (d, $J = 9.0$ Hz, 3 H), 8.05 (s, 2 H), 7.79 (d, $J = 7.8$ Hz, 4 H), 7.62–7.55 (m, 29 H), 7.42–7.35 (m, 21 H), 7.14–7.08 (m, 8 H). MS (MALDI-TOF): Calc. for $C_{152}H_{82}Br_8$: [M] 2547.51, found: [M+2] 2549.0.

Compound **18**: A mixture of dendron **17** (100 mg, 0.04 mmol), **9** (444 mg, 0.64 mmol), $Pd(PPh_3)_4$ (289 mg, 0.25 mmol) and $NaHCO_3$ (300 mg) in THF/H_2O (20 ml per 4 ml) was stirred at 70 °C for 15 days under nitrogen

atmosphere. After cooling to room temperature, brine (100 ml) was added, and the reaction solution was extracted with dichloromethane (40 ml × 3). The organic solvent was collected and dried with sodium sulfate. After the solvent was removed in vacuum, the obtained residue was further purified through silica gel column chromatography using methylene chloride/petroleum ether (v/v, 1:8) as the eluent to give **18** (light yellow solid, 55 mg, 21%). ^{1}H NMR (600 MHz, $CDCl_3$, 298 k): $\delta = 8.57$ (s, 7 H), 8.34 (s, 4 H), 8.30 (s, 4 H), 8.24–8.15 (m, 29 H), 8.02 (t, $J = 9.0$ Hz, 8 H), 7.86-7.81 (m, 43 H), 7.75 (d, $J = 6.0$ Hz, 9 H), 7.70–7.55 (m, 75 H), 7.51-7.41 (m, 36 H), 7.37–7.29 (m, 19 H), 1.14 (s, 36 H), 1.12 (s, 36 H), 1.07 (s, 36 H), 1.05 (s, 36 H). MS (MALDI-TOF): Calc. for $C_{504}H_{378}$: [M] 6428.96, found: [M+2] 6431.

Preparation of TPPh, TTPy, OTPy and TOPhP nanoparticles

TPPh in a stock THF (5.125 ml, 0.024 mM) solution was rapidly injected into ultrapure water (12 ml) under ultrasonic. After 5 min, the formed solution was bubbled with nitrogen for 1 h, and then the resulting solution was heated. After about 3 h, only 5 ml of water was observed. The nanoparticles were formed and characterized. Accordingly, the other nanoparticles of **TTPy**, **OTPy** and **TOPhP** were prepared at the same conditions.

Cytotoxicity assays

HeLa cells were cultured and seeded at a density of 5×10^3 cells per well in 96-well plates in Dulbecco's modified Eagle's medium incorporated 10% fetal bovine serum. After incubated overnight, the culture medium was replaced with 100 µl fresh cell culture medium containing various concentrations of nanoparticles. After 24-h incubation, the medium was replaced with 100 µl 0.5 mg ml^{-1} 3-(4′,5′-dimethylthiazol-2′-yl)-2,5-diphenyl-2H-tetrazolium hydrobromide (MTT) and incubated for 3 h at 37 °C. The MTT solution was discarded and then dissolved with 100 µl dimethyl sulfoxide. The absorbance at 570 nm was measured using Synergy HT microplate reader

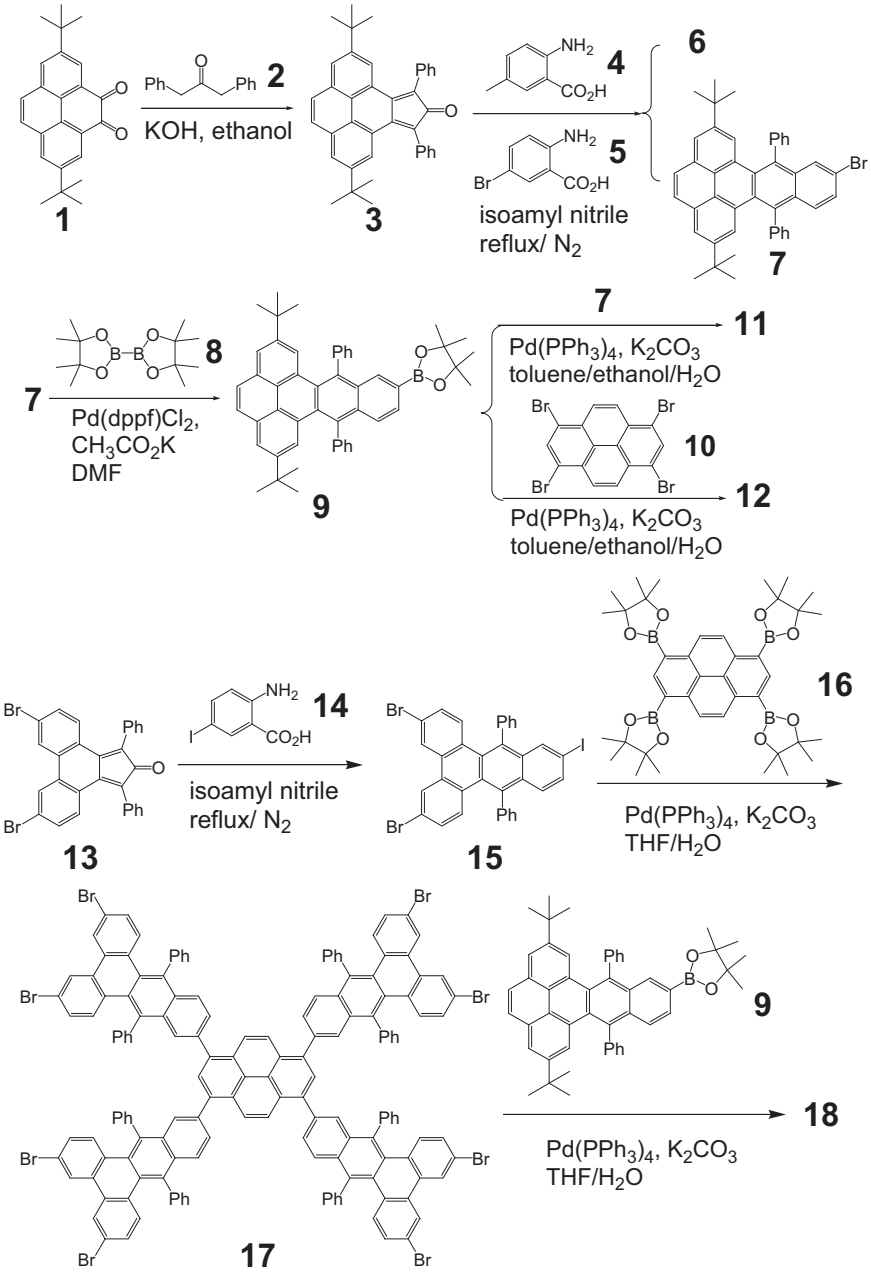

Figure 1 Synthetic route to **DBPy** (**6**), **DPyT** (**11**), **TTPy** (**12**) and **OTPy** (**18**).

(BioTek, Winooski, VT, USA). All experiments were conducted in triplicate and presented as mean ± s.d.

Photostability

To confirm the photostability, 25 μM nanoparticles solution were added dropwise on slide and then covered by coverslip. The samples were continuously irradiated by a mercury lamp (100 W) with 380/30 nm excitation filter (for **TPPh**, **TTPy** and **OTPy** nanoparticles) and 540/40 nm excitation filter (for **TOPhP** nanoparticles). Then fluorescence intensities were measured from Olympus IX 71, Tokyo, Japan, fluorescence microscopy with the software.

Cell imaging

HeLa cells were seeded at a density of 1×10^4 cells per well in 35-mm glass dishes. After incubation overnight, the cells were incubated with fresh culture medium containing various nanoparticles at a concentration of 1 μM for 18 h at 37 °C. Then the cells were washed with phosphate-buffered saline (pH = 7.4) and stained by nuclear localization dye (4′,6-diamidino-2-phenylindole (DAPI) or propidium iodide (PI)) for intracellular localization analysis. The cells were washed three times with phosphate-buffered saline again before recording by confocal laser scanning microscopy (FV1000-IX 81, Olympus, Tokyo, Japan).

RESULTS AND DISCUSSION

Synthesis

The synthetic approach to **DBPy**, **DPyT**, **TTPy** and **OTPy** is depicted in Figure 1. Note that compounds **TPPh**,[47] **13**,[48] **16**[49] and **TOPhP**[50] were prepared according to the reported methods. 2,7-Di-*tert*-butyl-pyrene-4,5-ketone[51] (**1**) was first reacted with commercially available 1,3-diphenylacetone (**2**) in the presence of potassium hydroxide and ethanol to give black solid **3**, which was further converted to **6** (**DBPy**) and **7** in 11% and 28% isolated yield through a Diels-Alder [4+2] cycloaddition reaction by treatment with 2-amino-5-methylbenzoic acid (**4**), 2-amino-5-bromobenzoic acid (**5**) and isoamyl nitrile in refluxing DCE. Bromo-substituted derivative **7** was converted into the corresponding single pinacol boronic ester (**9**) under Pd(dppf)Cl_2, dry KOAc and bis(pinacolato)diboron (**8**). The Suzuki coupling between the intermediate **9** and **7**/1,3,6,8-tetrabromopyrene (**10**) using Pd$(PPh_3)_4$ and K_2CO_3 as the catalysts in THF/water or toluene/ethanol/water solution afforded the target molecules **11** (**DPyT**) and **12** (**TTPy**) in 68% and 45% yield, respectively. Compound **15** (81%) was generated from **13** and 2-amino-5-iodobenzoic acid (**14**) by treatment with isoamyl nitrile in DCE at 90 °C, which was selectively reacted with **16** to afford **17** in 37% yield. Under the similar Suzuki reaction, the larger dendrimer **18** (21%) was successfully achieved through the further cross-coupling of **17** and **9**. The introduction of *tert*-butyl groups and twisted structures in **DBPy**, **DPyT**, **TPPh** and **OTPy** made them easily dissolve in common organic solvents such as toluene, 1,2-dichlorobenzene, dichloromethane, chloroform and THF, which was in favor of full characterization through ^{1}H NMR, ^{13}C NMR, MALDI-TOF (or EI) mass spectroscopes (Supplementary Figures S3–S27).

Single crystal for compound DBPy

The twisted structure was confirmed by X-ray diffraction analysis. Single crystals of **DBPy**, **DPyT**, **TTPy** and **OTPy** were grown through slow evaporation of a mixture solution of CH_2Cl_2/methanol, and the formed crystals of **DBPy** were suitable for the test. The molecular structure of **DBPy** and its packing model are shown in Figure 2 and the detailed crystal data are presented in Supplementary Table S1. **DBPy** adopts a triclinic unit cell, space group P-1 (CCDC number: 999488) and the crystal parameter data are $a = 15.5265$ (14) Å, $b = 10.2258$ (9) Å, $c = 20.7939$ (18) Å, $\alpha = 90°$, $\beta = 98.997$ (2)°, $\gamma = 90°$. In the molecular structure, the terminal pyrene unit is almost coplanar, and the near naphthalene moiety is twisted out of this plane, which was similar to our reported molecules.[35–40] It should be noted that the twisted torsion angle of plane C1-C2-C24 and plane C10-C12-C14 is 27.69°. Furthermore, the intermolecular distance is more than 3.8 Å, inferring that π–π stacking interaction is absent between intermolecules based on the packing model (Figure 2b). This distortion model was in favor of decreasing the aggregation in the solid state. Taking **TPPh**, **TTPy**, **OTPy** and **TOPhP** into consideration, one do believe that the twisted structures and three-dimensional architectures could effectively suppress π–π interaction, which might be beneficial to decreasing the fluorescent quenching in the self-assembled aggregation to a great extent. Thermal gravimetric analysis was measured under nitrogen atmosphere, and the onset of 5% weight loss of **DBPy**, **DPyT**, **TPPh**,[48] **TTPy**, **OTPy** and **TOPhP** are 386, 467, 232, 325, 246 and 181 °C, respectively, indicating that the obtained compounds have high thermal stability (Supplementary Figure S1).

Fabrication and characterization of organic nanoparticles

The nanoparticles of **TPPh**, **TTPy**, **OTPy** and **TOPhP** were prepared by using a re-precipitation method.[52,53] Compounds **TPPh–TOPhP**

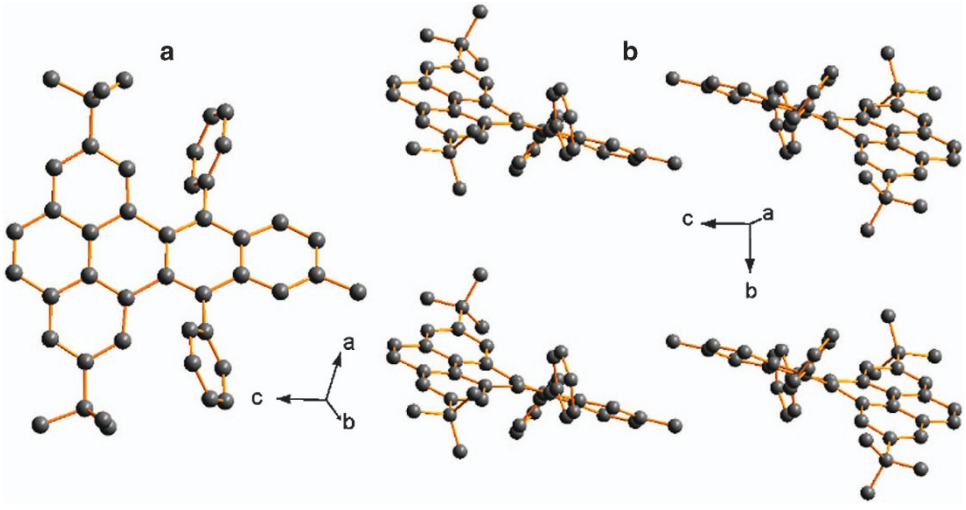

Figure 2 (**a**) Single crystal of **DBPy** and (**b**) its corresponding packing model.

dissolved in THF solution were quickly injected into pure water under sonication. The resulting nanoparticles were subsequently deposited on silica wafers and characterized by FESEM. It should be pointed out that the obtained nanoparticles can remain suspended in water solution. In comparison, under the similar condition, both **DBPy** and **DPyT** emitted strong blue light in water, and disordered aggregation was observed. This confirms that the twisted structure and three-dimensional architecture might be beneficial for the formation of nanoparticles. As shown in Figure 3, the formed nanoparticles are spherical shapes with the diameters of 60–200 nm for **TPPh**, 40–120 nm for **TTPy**, 150–500 nm for **OTPy** and 76–300 nm for **TOPhP**. Moreover, hydrodynamic diameters of **TPPh** (102 nm), **TTPy** (204 nm), **OTPy** (169 nm) and **TOPhP** (81 nm), determined by using dynamic light scanning, are close to those from SEM analysis (Figure 3 and Supplementary Table S2). Zeta potentials (ζ) of the nanoparticles solutions were observed to be −36.6 mV for **TPPh** nanoparticles, −1.7 mV for **TTPy** nanopartices, −29.3 mV for **OTPy** nanoparticles and −25.6 mV for **TOPhP** nanoparticles, implying that the surface of the nanoparticles were negatively charged.

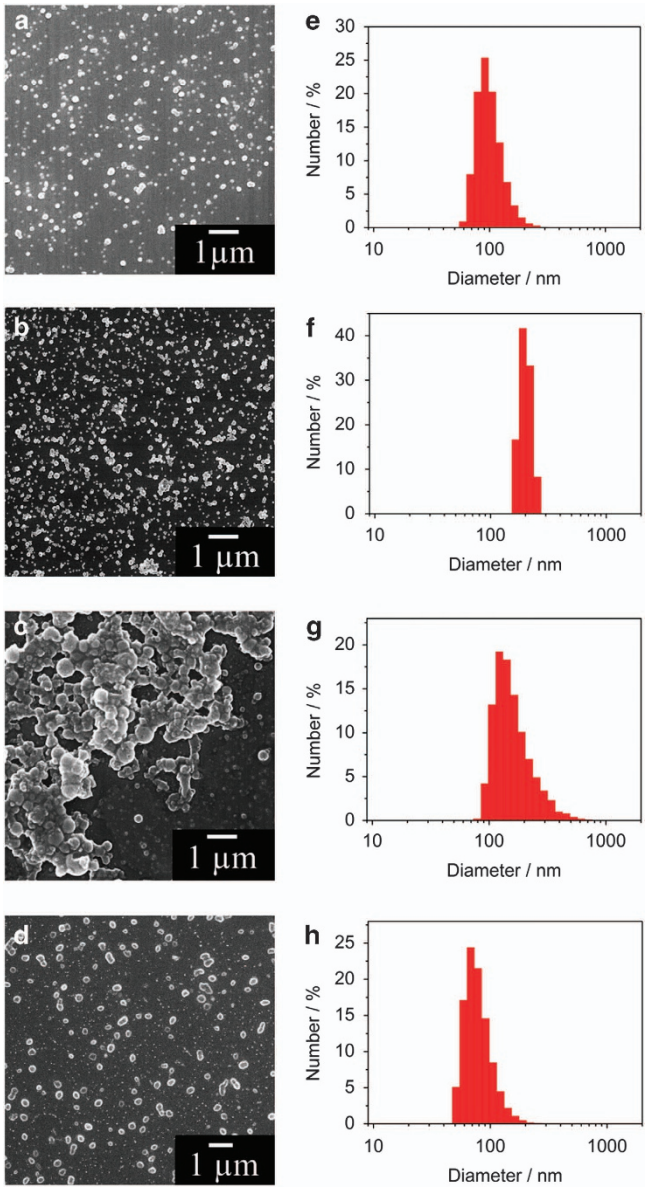

Figure 3 SEM images of **TPPh** (**a**), **TTPy** (**b**), **OTPy** (**c**) and **TOPhP** (**d**) nanoparticles. The hydrodynamic diameters of **TPPh** (**e**), **TTPy** (**f**), **OTPy** (**g**) and **TOPhP** (**h**) nanoparticles recorded by using dynamic light scattering.

Optical property

The optical properties of the obtained molecules in THF solution and their corresponding nanoparticles in pure water were investigated, and the results are shown in Figure 4 and Supplementary Figure S2. Small dendron **TPPh** in THF displayed the maximum absorption band at 350 nm, with other two peaks at 336 nm and 430 nm owing to the π–π^* transition. **TPPh** in THF showed azure fluorescence with the emission maximum at 445 and 470 nm. When the central unit benzene was substituted with pyrene unit, the formed compound **TTPy** presented broad absorption peak at 350 and 414 nm, which might be assigned to the increase of conjugated length. More interesting, **TTPy** exhibited strong emission at 484 nm, falling into the cyan-emission region. The larger dendron **OTPy** showed a broad structureless absorption between 320 and 480 nm, with a maximum around 380 nm and emission peak at 490 nm. Note that it also emits cyan light in THF solution. The known compound **TOPhP** exhibited the absorption bands at 575, 533 and 442 nm. The red emission spectra of **TOPhP** displayed structured features with the maximum peak at 608 nm and a shoulder peak at 655 nm. In addition, the quantum yields of **TPPh**, **TTPy**, **OTPy** and **TOPhP** were calculated to 0.35, 0.82, 0.79 and 0.80, respectively, by using 9,10-diphenylanthracene ($\Phi_f = 0.95$ in ethanol) or *N*,*N*′-di(2,6-diisopropylphenyl)-perylene-3,4:9:10-tetracarboxylic acid bisimide ($\Phi_f = 1.00$ in chloroform) as the standards.[54,55]

The photophysical properties of the desired nanoparticles in pure water were further measured. **TPPh**, **TTPy** and **TOPhP** nanoparticles presented the similar absorption profiles compared with those in diluted THF solution. However, **OTPy** nanoparticles showed the same absorption maximum at 380 nm but much broader absorption contour than that in THF, which might result from the weak electronic coupling of molecule **OTPy**.[56,57] As shown in Figure 4g, a 27-nm bathochromic shift in fluorescence spectra was observed between **TTPy** (484 nm) and **OTPy** nanoparticles (511 nm), which was larger than that (6 nm) in THF. More importantly, one can notice that the full width at half maximum became smaller than those in THF. Apparently, **TPPh**, **TTPy**, **OTPy** and **TOPhP** nanoparticles in pure water emitted blue, cyan, green and red color with the quantum yields of 0.11, 0.10, 0.04 and 0.06 (Figure 4h), respectively, inferring that they might be applied in realization of all the visible emission region and special imaging of living cells.

Photostability and cytotoxicity

The photostability and cytotoxicity of the obtained nanoparticles were examined to assess their potential application in biology. As shown in Figure 5a, the nanoparticles in aqueous solutions retained the emission intensity of about 60–80% under continuous irradiation for 60 s, indicating good photostability. **TPPh** and **TTPy** nanoparticles exhibited negligible cytotoxicity recorded by an MTT assay (Figure 5b). **OTPy** and **TOPhP** nanoparticles showed small cell cytotoxicity in the concentration of < 1.0 μM, which can meet the standard for the test in the cell imaging.

Cell imaging

In light of the above facts, the cellular imaging *in vitro* based on these nanoparticles was further investigated by using confocal laser scanning microscope where red fluorescence PI was selected as the nucleus-located dyes for **TPPh**, **TTPy** and **OTPy** nanoparticles and blue

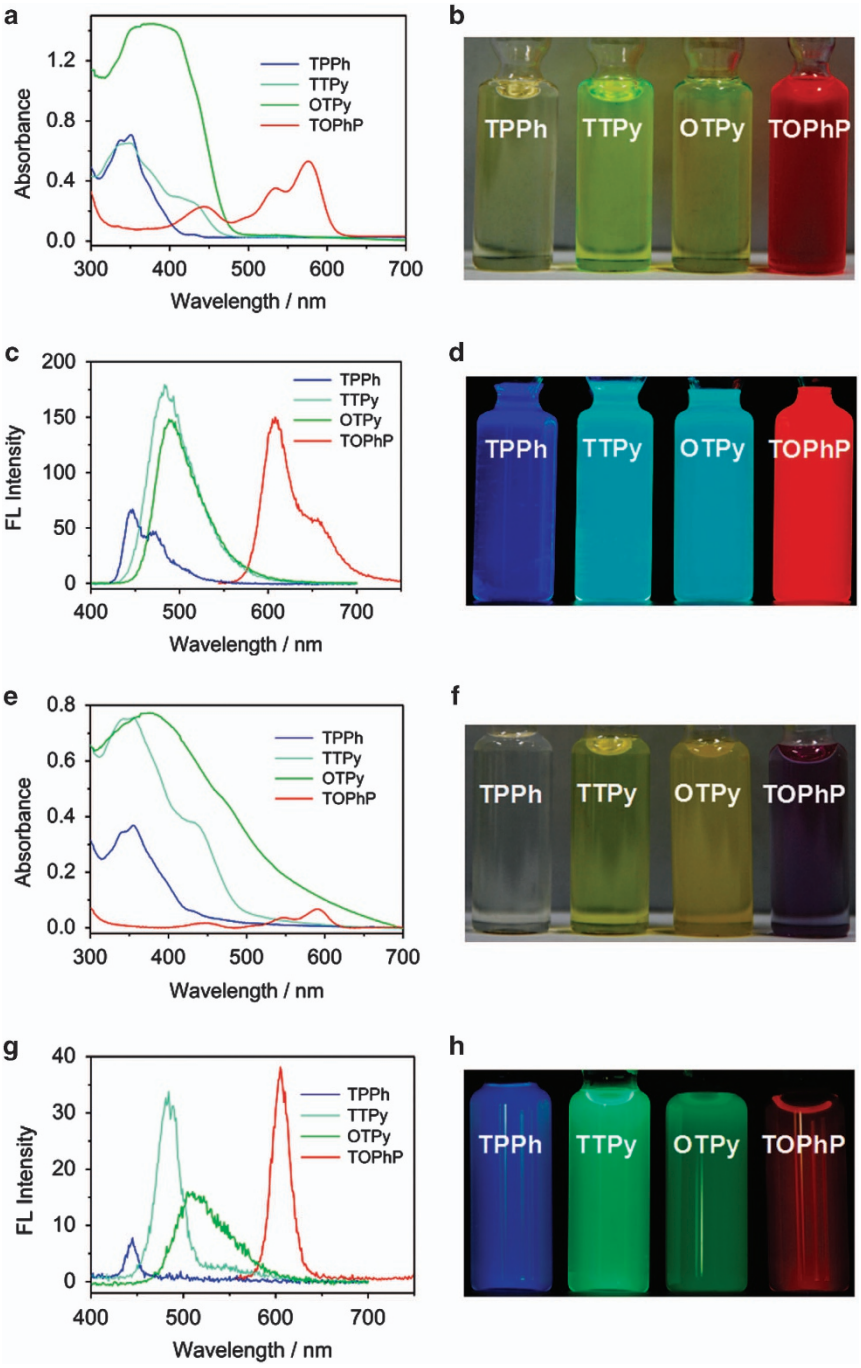

Figure 4 (**a**) UV-Vis absorption and (**c**) fluorescence spectra of **TPPh**, **TTPy**, **OTPy** and **TOPhP** in THF (1×10^{-5} M) solution. (**e**) Absorption spectra and (**g**) fluorescence spectra of **TPPh**, **TTPy**, **OTPy** and **TOPhP** nanoparticles in water. Panels (**b**) and (**f**) show the corresponding absorption colors in THF and water, panels (**d**) and (**h**) show the corresponding emission colors in THF and water under the UV light ($\lambda = 365$ nm).

fluorescence DAPI was utilized for **TOPhP** nanoparticles. The results are depicted in Figure 6. **TTPy** nanoparticles concentrated on the membrane of HeLa cells, while the other three nanoparticles are mainly observed in the cytoplasms. This might result from the small zeta potential (−1.7 mV) of **TTPy** nanoparticle solution. These particles were prone to agglomerate, which was a disadvantage to penetrate into the membrane.[58,59] Accordingly, **TPPh**, **OTPy** and **TOPhP** nanoparticles having high potential values could be stained to cytoplasm areas owing to endocytosis. Clearly, the desired nanoparticles could selectively be stained in the special cellular position, which is beneficial for the location, diagnostic and prognostic bio-information for pathologists.

In summary, we have synthesized and characterized a family of π-conjugated dendrimers containing branched twistacenes. Molecular structures can significantly affect the size and shape of the aggregation that fabricated through re-precipitation method. Interestingly, the formed nanoparticles kept strong blue, cyan, green and red luminescence in aqueous solution compared with their THF solution. As a new class of detection systems, the self-assembled multicolor nanoparticles could selectively flow into the membrane and cytoplasm

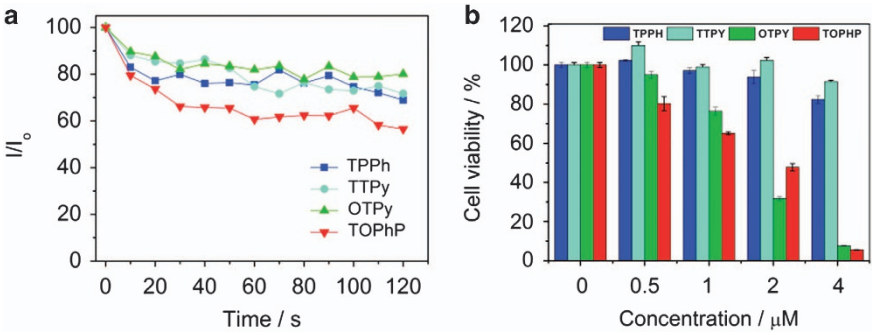

Figure 5 (**a**) Photostability of **DBPy**, **TTPy**, **OTPy** and **TOPhP** nanoparticles upon irradiation at 380 and 455 nm. (**b**) Viability of HeLa cells in the presence of the obtained nanoparticles with an MTT assay.

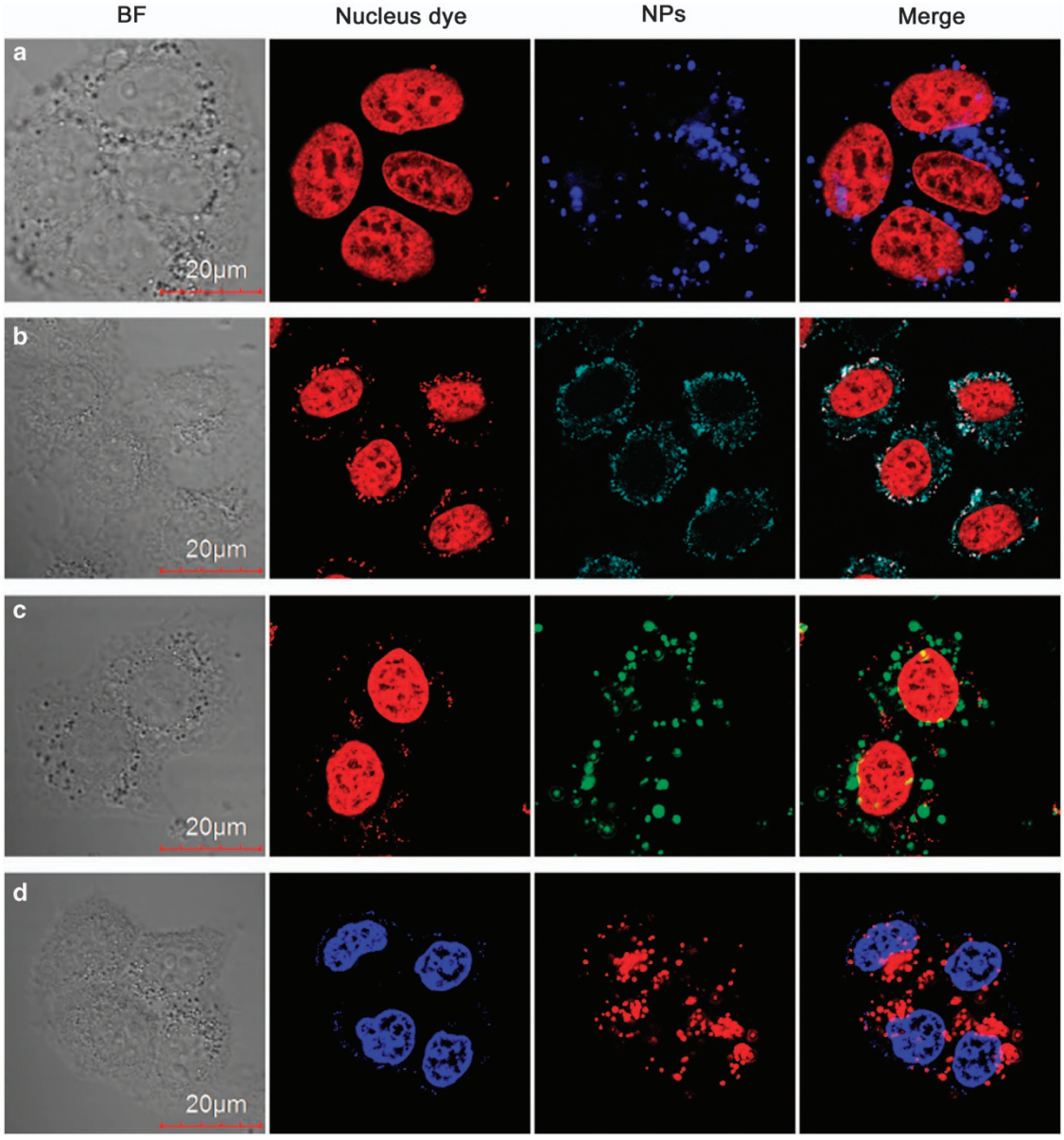

Figure 6 Fluorescence images of HeLa cells treated with **TPPh** (**a**), **TTPy** (**b**), **OTPy** (**c**) and **TOPhP** (**d**) nanoparticles.

of HeLa cells, being indicative of feasibility and efficiency in cell fluorescent imaging. Obviously, our systematic study of these molecules could provide more room to rational design and functionality of the larger dendrimers. Pursuing the nanoparticles with low cytotoxicity and high photostability based on all-carbon conjugated dendrons and potential application in biological processes are on the way.

CONFLICT OF INTEREST

The authors declare no conflict of interest.

ACKNOWLEDGEMENTS

We thank the National Natural Science Foundation of China (21102031 and 21442010), the Natural Science Foundation of Hebei Province (B2014201007) and the introduction of overseas students foundation of Hebei Province (C2012003048) for financial support.

1 Hoeben, F. J. M., Jonkheijm, P., Meijer, E. W. & Schenning, A. P. H. About supramolecular assemblies of π-conjugated systems. *Chem. Rev.* **105**, 1491–1546 (2005).
2 Babu, S. S., Praveen, V. K. & Ajayaghosh, A. Functional π-gelators and their applications. *Chem. Rev.* **114**, 1973–2129 (2014).
3 Li, Y., Liu, T., Liu, H., Tian, M. & Li, Y. Self-assembly of intramolecular charge-transfer compounds into functional molecular systems. *Acc. Chem. Res.* **47**, 1186–1198 (2014).
4 Zheng, H., Li, Y., Liu, H., Yin, X. & Li, Y. Construction of heterostructure materials toward functionality. *Chem. Soc. Rev.* **40**, 4506–4524 (2011).
5 Liu, H., Xu, J., Li, Y. & Li, Y. Aggregate nanostructures of organic molecular materials. *Acc. Chem. Res.* **43**, 1496–1508 (2010).
6 Xiao, J., Xiao, X., Zhao, Y., Wu, B., Liu, Z., Zhang, X., Wang, S., Zhao, X., Liu, L. & Jiang, L. Synthesis, physical properties and self-assembly behavior of azole-fused pyrene derivatives. *Nanoscale* **5**, 5420–5425 (2013).
7 Pho, T. V., Toma, F. M., Chabinyc, M. L. & Wudl, F. Self-assembling decacyclene triimides prepared through a regioselective hextuple friedel–crafts carbamylation. *Angew. Chem. Int. Ed.* **52**, 1446–1451 (2013).
8 Xiao, J., Yin, Z., Li, H., Zhang, Q., Boey, F., Zhang, H. & Zhang, Q. Postchemistry of organic particles: When TTF microparticles meet TCNQ microstructures in aqueous solution. *J. Am. Chem. Soc.* **132**, 6926–6928 (2010).
9 Ortony, J. H., Chatterjee, T., Garner, L. E., Chworos, A., Mikhailovsky, A., Kramer, E. J. & Bazan, G. C. Self-assembly of an optically active conjugated oligoelectrolyte. *J. Am. Chem. Soc.* **133**, 8380–8387 (2011).
10 Feng, L., Zhu, C., Yuan, H., Liu, L., Lv, F. & Wang, S. Conjugated polymer nanoparticles: preparation, properties, functionalization and biological applications. *Chem. Soc. Rev.* **42**, 6620–6633 (2013).
11 Wu, C. & Chiu, D. T. Highly fluorescent semiconducting polymer dots for biology and medicine. *Angew. Chem. Int. Ed.* **52**, 3086–3109 (2013).
12 Wang, F., Liu, Z., Wang, B., Feng, L., Liu, L., Lv, F., Wang, Y. & Wang, S. Multi-colored fibers by self-assembly of DNA, histone proteins, and cationic conjugated polymers. *Angew. Chem. Int. Ed.* **53**, 424–428 (2014).
13 Wu, C., Schneider, T., Zeigler, M., Yu, J., Schiro, P G., Burnham, D. R., McNeill, J. D. & Chiu, D. T. Bioconjugation of ultrabright semiconducting polymer dots for specific cellular targeting. *J. Am. Chem. Soc.* **132**, 15410–15417 (2010).
14 Feng, G., Li, K., Liu, J., Ding, D. & Liu, B. Bright single-chain conjugated polymer dots embedded nanoparticles for long-term cell tracing and imaging. *Small* **10**, 1212–1219 (2014).
15 Anees, P., Sreejith, S. & Ajayaghosh, A. Self-assembled near-infrared dye nanoparticles as a selective protein sensor by activation of a dormant fluorophore. *J. Am. Chem. Soc.* **136**, 13233–13239 (2014).
16 Gill, M. R., Lara-Garcia, J., Foster, S. J., Smythe, C., Battaglia, G. & Thomas, J. A. A ruthenium(II) polypyridyl complex for direct imaging of DNA structure in living cells. *Nat. Chem.* **1**, 662–667 (2009).
17 Chan, Y. S., Ye, F., Gallina, M. E., Zhang, X., Jin, Y., Wu, I. C. & Chiu, D. T. Hybrid semiconducting polymer dot–quantum dot with narrow-band emission, near-infrared fluorescence, and high brightness. *J. Am. Chem. Soc.* **134**, 7309–7312 (2012).
18 Zeigler, M. B., Sun, W., Rong, Y. & Chiu, D. T. Hybrid semiconducting polymer nanoparticles as polarization-sensitive fluorescent probes. *J. Am. Chem. Soc.* **135**, 11453–11456 (2013).
19 Thomas, A. W., Henson, Z. B., Du, J., Vandenberg, C. A. & Bazan, G. C. Synthesis, characterization, and biological affinity of a near-infrared-emitting conjugated oligoelectrolyte. *J. Am. Chem. Soc.* **136**, 3736–3739 (2014).
20 Kim, H. J., Heo, C. H. & Kim, H. M. Benzimidazole-based ratiometric two-photon fluorescent probes for acidic pH in live cells and tissues. *J. Am. Chem. Soc.* **135**, 17969–17977 (2013).
21 Li, M., Feng, L., Lu, H., Wang, S. & Chen, C. Tetrahydro[5]helicene-based nanoparticles for structure-dependent cell fluorescent imaging. *Adv. Funct. Mater.* **24**, 4405–4412 (2014).
22 Pu, K., Li, K., Zhang, X. & Liu, B. Conjugated oligoelectrolyte harnessed polyhedral oligomeric silsesquioxane as light-up hybrid nanodot for two-photon fluorescence imaging of cellular nucleus. *Adv. Mater.* **22**, 4186–4189 (2010).
23 Depan, D. & Misra, R. D. K. Structural and physicochemical aspects of silica encapsulated ZnO quantum dots with high quantum yield and their natural uptake in HeLa cells. *J. Biomed. Mater. Res. Part A* **102A**, 2934–2941 (2014).
24 Jia, Z. & Misra, R. D. K. Tunable ZnO quantum dots for bioimaging: synthesis and photoluminescence. *Mater. Tech. Adv. Perf. Mater.* **28**, 221–227 (2013).
25 Chandrasekaran, S. & Misra, R. D. K. Phtonic antioxidant ZnS (Cd) nanorod synthesis for drug carrier and bioimaging. *Mater. Tech. Adv. Perf. Mater.* **28**, 228–232 (2013).
26 Clar, E. *Polycyclic Hydrocarbons*, (Academic Press, London, UK, 1964).
27 Bendikov, M., Wudl, F. & Perepichka, D. Tetrathiafulvalenes, oligoacenenes, and their buckminsterfullerene derivatives: the brick and mortar of organic electronics. *Chem. Rev.* **104**, 4891–4946 (2004).
28 Kaur, I., Jazdzyk, M., Stein, N. N., Prusevich, P. & Miller, G. P. Design, synthesis, and characterization of a persistent nonacene derivative. *J. Am. Chem. Soc.* **132**, 1261–1263 (2010).
29 Purushothaman, B., Bruzek, M., Parkin, S. R., Miller, A. F. & Anthony, J. E. Synthesis and structural characterization of crystalline nonacenes. *Angew. Chem. Int. Ed.* **50**, 7013–7017 (2011).
30 Parkhurst, R. R. & Swager, T. M. Synthesis and optical properties of phenylene-containing oligoacene. *J. Am. Chem. Soc.* **134**, 15351–15356 (2012).
31 Watanabe, M., Chang, Y. J., Liu, S. W., Chao, T. H., Goto, K., Islam, M. M., Yuan, C. H., Tao, Y. T., Shinmyozu, T. & Chow, T. J. The synthesis, crystal structure and charge-transport properties of hexacene. *Nat. Chem.* **4**, 574–578 (2012).
32 Pascal, R. A. Jr Twisted acenes. *Chem. Rev.* **106**, 4809–4819 (2006).
33 Xiao, J., Liu, Z., Zhang, X., Wu, W., Ren, T., Lv, B., Jiang, L., Wang, X., Chen, H., Su, W. & Zhao, J. Substituent effects in twisted dibenzotetracene derivatives: blue emitting materials for organic light-emitting diodes. *Dyes Pigments* **112**, 176–182 (2015).
34 Li, J. & Zhang, Q. Mono- and oligocyclic aromatic ynes and diynes as building blocks to approach larger acenes, heteroacenes, and twistacenes. *Synlett* **24**, 686–696 (2013).
35 Xiao, J., Duong, H. M., Liu, Y., Shi, W., Ji, L., Li, G., Li, S., Liu, X., Ma, J., Wudl, F. & Zhang, Q. Synthesis and structure characterization of a stable nonatwistacene. *Angew. Chem. Int. Ed.* **51**, 6094–6098 (2012).
36 Xiao, J., Liu, S., Liu, Y., Ji, L., Liu, X., Zhang, H., Sun, X. & Zhang, Q. Synthesis, structure, and physical properties of 5,7,14,16-tetraphenyl-8:9,12:13-bisbenzo-hexatwistacene. *Chem. Asian J.* **7**, 561–564 (2012).
37 Xiao, J., Malliakas, C. D., Liu, Y., Zhou, F., Li, G., Su, H., Kanatzidis, M. G., Wudl, F. & Zhang, Q. "Clean reaction" strategy to approach a stable, green heptatwistacene containing a single terminal pyrene unit. *Chem. Asian J.* **7**, 672–675 (2012).
38 Xiao, J., Divayana, Y., Zhang, Q., Doung, H. M., Zhang, H., Boey, F., Sun, X. & Wudl, F. Synthesis, structure, and optoelectronic properties of a new twistacene 1,2,3,4,6,13-hexaphenyl-7:8,11:12-bisbenzo-pentacene. *J. Mater. Chem.* **20**, 8167–8170 (2010).
39 Zhang, Q., Divayana, Y., Xiao, J., Wang, Z., Tiekink, E. R. T., Doung, H.M., Zhang, H., Boey, F., Sun, X. & Wudl, F. Synthesis, characterization, and bipolar transporting behavior of a new twisted polycyclic aromatic hydrocarbon: 1',4'-diphenyl-naphtho-(2'.3':1.2)-pyrene-6'-nitro-7'-methyl carboxylate. *Chem. Eur. J.* **16**, 7422–7426 (2010).
40 Liu, Z., Wang, W., Wu, W., Chen, H., Zhang, X., Ren, T., Wang, X., Zhao, J. & Xiao, J. Synthesis, characterization and photocurrent behavior of asymmetrical heterotwistacenes. *Dyes Pigments* **115**, 143–148 (2015).
41 Weil, T., Vosch, T., Hofkens, J., Peneva, K. & Müllen, K. The rylene colorant family—tailored nanoemitters for photonics research and applications. *Angew. Chem. Int. Ed.* **49**, 9068–9093 (2010).
42 Qin, T., Zhou, G., Scheiber, H., Bauer, R. E., Baumgarten, M., Anson, C. E., List, E. J. W. & Müllen, K. Polytriphenylene dendrimers: a unique design for blue-light-emitting materials. *Angew. Chem. Int. Ed.* **47**, 8292–8296 (2008).
43 Qin, T., Wiedemair, W., Nau, S., Trattnig, R., Sax, S., Winkler, S., Vollmer, A., Koch, N., Baumgarten, M., List, E. J. W. & Müllen, K Core, shell, and surface-optimized dendrimers for blue light-emitting diodes. *J. Am. Chem. Soc.* **133**, 1301–1303 (2011).
44 Wang, J., Yan, J., Tang, Z., Xiao, Q., Ma, Y. & Pei, J. Gradient shape-persistent π-conjugated dendrimers for light-harvesting: synthesis, photophysical properties, and energy funneling. *J. Am. Chem. Soc.* **130**, 9952–9962 (2008).
45 Wang, J., Luo, J., Liu, L., Zhou, Q, Ma, Y. & Pei, J. Nanosized gradient π-conjugated thienylethynylene dendrimers for light harvesting: synthesis and properties. *Org. Lett.* **8**, 2281–2284 (2006).
46 Wang, J., Tang, Z., Xiao, Q., Ma, Y. & Pei, J. Star-shaped D-π-A conjugated molecules: synthesis and broad absorption bands. *Org. Lett.* **11**, 863–866 (2009).
47 Liu, Z., Xiao, J., Fu, Q., Feng, H., Zhang, X., Ren, T., Wang, S., Ma, D., Wang, X. & Chen, H. Synthesis and physical properties of the conjugated dendrons bearing twisted acenes used in solution processing of organic light-emitting diodes. *ACS Appl. Mater. Interfaces* **5**, 11136–11141 (2013).
48 Schwab, M. G., Qin, T., Pisula, W., Mavrinskiy, A., Feng, X., Baumgarten, M., Kim, H., Laquai, F., Schub, S., Trattnig, R., List, E. J. W. & Müllen, K. Molecular triangles: synthesis, self-assembly, and blue emission of cyclo-7,10-tris-triphenylenyl macrocycles. *Chem. Asian J.* **6**, 3001–3011 (2011).

49 Hammer, B. A. G., Baumqarten, M. & Müllen, K. Covalent attachment and release of small molecules from functional polyphenylene dendrimers. *Chem. Commun.* **50**, 2034–2036 (2014).
50 Hofkens, J., Vosch, T., Maus, M., Köhn, F., Cotlet, M., Weil, T., Herrmann, A., Müllen, K. & De Schryver, F. C. Conformational rearrangements in and twisting of a single molecule. *Chem. Phys. Lett.* **333**, 255–263 (2001).
51 Hu, J., Zhang, D. & Harris, F. W. Ruthenium(III) chloride catalyzed oxidation of pyrene and 2,7-disubstitued pyrenes: an efficient, one-step synthesis of pyrene-4,5-diones and pyrene-4,5,9,10-tetraones. *J. Org. Chem.* **70**, 707–708 (2005).
52 Tao, Z., Hong, G., Shinji, C., Chen, C., Diao, S., Antaris, A. L., Zhang, B., Zou, Y. & Dai, H. Biological imaging using nanoparticles of small organic molecules with fluorescence emission at wavelengths longer than 1000 nm. *Angew. Chem. Int. Ed.* **52**, 13002–13006 (2013).
53 Wu, C., Szymanski, C. & McNeill, J. Preparation and encapsulation of highly fluorescence conjugated polymer nanoparticles. *Langmuir* **22**, 2956–2960 (2006).
54 Zhang, H., Hong, X., Ba, X., Yu, B., Wen, X., Wang, S., Wang, X., Liu, L. & Xiao, J. Synthesis, physical properties, and photocurrent behavior of strongly emissive boron-chelate heterochrysene derivatives. *Asian J. Org. Chem.* **3**, 1168–1172 (2014).
55 Xiao, J., Xu, J., Cui, S., Liu, H., Wang, S. & Li, Y. Supramolecula helix of an amphiphilic pyrene derivatives induced by chiral tryptophan through electrostatic interactions. *Org. Lett.* **10**, 645–648 (2008).
56 Balakrishnan, K., Datar, A., Naddo, T., Huang, J., Oitker, R., Yen, M., Zhao, J. & Zang, L. Effect of side-chain substituents on self-assembly of perylene diimide molecules: morphology control. *J. Am. Chem. Soc.* **128**, 7390–7398 (2006).
57 Gong, X., Milic, T., Xu, C., Battas, J. D. & Drain, C. M. Preparation and characterization of porphyrin nanoparticles. *J. Am. Chem. Soc.* **124**, 14290–14291 (2002).
58 Vijayakumar, C., Sugiyasu, K. & Takeuchi, M. Oligofluorene-based electrophoretic nanoparticles in aqueous medium as a donor scaffold for fluorescence resonance energy transfer and white-light emission. *Chem. Sci.* **2**, 291–294 (2011).
59 Wang, Y., Jones, E. M., Tang, Y., Ji, E., Lopez, G. P., Chi, E. Y., Schanze, K. S. & Whitten, DG Effect of polymer chain length on membrane perturbation activity of cationic phenylene ethynylene oligomers and polymers. *Langmuir* **27**, 10770–10775 (2011).

Supplementary Information accompanies the paper on the NPG Asia Materials website (http://www.nature.com/am)